Electric field-treated MEAs for improved fuel cell performance

Zhi-Tao Wang[a,b], Yu-Xin Wang[a,b], Li Xu[a,*], Qi-Jun Gao[a,b], Guo-Qiang Wei[a,b], Jun Lu[a,b]

[a] *School of Chemical Engineering and Technology, Tianjin University, Weijin Road 92, Tianjin 300072, China*
[b] *United State Key Lab of Chemical Engineering, Tianjin University, Weijin Road 92, Tianjin 300072, China*

ARTICLE INFO

ABSTRACT

In this paper, electric field assisted fabrication of membrane electrode assemblies (MEAs) for fuel cells is proposed, with the aim of improving the electronic and ionic connections in the catalyst layers and increasing the efficiency of catalyst utilization. Anodic and cathodic electrodes have been prepared by the perpendicular application of a low-frequency ac electric field to the catalyst ink spread on the surface of a gas diffusion layer (GDL) while the ink is drying. The thus prepared electrodes were hot-pressed onto a Nafion membrane to form the MEAs. Direct methanol fuel cells (DMFCs) with the electric field-treated MEAs (E-MEA) showed a substantial improvement in performance as compared with common MEAs (C-MEA) without electric field treatment. Under the same operating conditions, the maximum power density of a DMFC was increased from 42.3 to 60.0 mW cm^{-2} when a C-MEA was replaced by an E-MEA treated with a 5000 V cm^{-1} and 0.1 Hz ac electric field. Electrochemical impedance spectroscopy (EIS) measurements have shown that the through-plane ohmic resistances in the E-MEAs are lower than that in the C-MEA, while both the electronic and ionic resistances of the catalyst layer in the in-plane direction are higher for the E-MEAs, suggesting the formation of an oriented structure in the catalyst layers under the electric field treatment. EIS measurements have also shown that both the total reaction resistance and the anode reaction resistance in the E-MEAs are lower than in the C-MEA. Based on cyclic voltammetry (CV) data, it has been shown that Pt utilization in the cathode reaches a maximum of 62% for the E-MEA, as opposed to 37% for the C-MEA.

1. Introduction

Proton exchange membrane fuel cells (PEMFCs), including DMFCs, have attracted increasing attention in recent years as alternative mobile and portable power sources owing to their outstanding advantages, such as high efficiency, high power density, low or zero emissions, and reliability [1–3]. One of the key components of a PEMFC is the membrane electrode assembly (MEA), which consists of a proton exchange membrane (PEM), such as a Nafion® membrane, sandwiched between two catalyst layers serving as anodic electrode and cathodic electrode, respectively. Each catalyst layer, in which electrochemical reactions take place, is generally composed of three phases, namely a catalyst electronic conductive phase, a polyelectrolyte ionic conductive phase, and a void pores phase. These three phases are usually distributed randomly in the catalyst layer.

Many efforts have been focused on optimization of the electrode composition and structure in MEAs, in order to reduce the charge- and mass-transfer resistance and to extend effective utilization of the catalyst. Kim et al. [4] investigated how anode ionomer content affects the MEA performance in DMFCs. They showed that an anode with a supported catalyst generally requires considerably higher amounts of ionomer to function properly as compared to one with an unsupported catalyst. Fernandez et al. [5] studied the effects of solvent composition in the catalyst ink and evaporation rate on the microstructure of the catalytic layer. They showed that the structure and performance of the catalytic layer in an MEA are remarkably affected by the viscosity and dielectric constant of the solvent used to disperse both the catalyst and the Nafion ionomer. Liu and Wang [6] compared the performances of DMFCs with cathodes prepared by different methods. The MEAs with catalyst-coated-membrane (CCM) cathodes were found to have higher open-circuit voltages and larger limiting current densities, whereas catalyzed-diffusion-media (CDM) cathodes showed better performance at moderate current densities. The difference in performance between the CCM and CDM cathodes was explained in terms of their structural characteristics. Du et al. [7] conducted a parametric study of an ideally structured cathode catalyst layer in a PEMFC by means of a computer simulation. The cathode current density optimization at a given electrode potential was presented with respect to the nano-thread radius, porosity, platinum mass percentage, thickness, Nafion volume fraction, and

* Corresponding author. Tel.: +86 22 27890515; fax: +86 22 27890515.
E-mail address: xuli620@eyou.com (L. Xu).

platinum loading of the catalyst layer. Their simulation results suggested that the performance of the structured cathode strongly depends on the catalyst layer thickness, the Nafion volume fraction, and the platinum loading. It is noticeable that earlier studies were concerned more with catalyst layer composition, but that more attention has been paid to catalyst layer structure in recent years.

It has long been known that particles tend to form "pearl-chains" under the influence of an electric field [8]. Although there have already been a few research works on preparing aligned or oriented structures in various conductive membranes by utilizing an electric field as the driving force [9–12], Middelman [13] was the first to report the fabrication of oriented MEA electrodes for PEMFCs by using an electric field. While very impressive SEM images of highly structured catalyst layers were given and nearly 100% utilization of the catalyst was claimed in his report, little information was provided on the electrode preparation and performance, except "applying sufficiently strong electric field" and "cell voltage increases of up to 20%". To the best of our knowledge, no other works have hitherto been reported on enhancing MEA performance through electric field treatment.

In this paper, we report our research on preparing MEAs with electrodes treated by ac electric fields of varying frequencies. The performance of the E-MEAs thus prepared was compared with that of C-MEA in a single-cell DMFC. The E-MEAs, as well as single electrodes, were also characterized by EIS, CV, and SEM methods in order to determine the changes in the E-MEAs resulting from electric field treatment.

2. Experimental

2.1. MEA preparation

Pt-Ru/C (20 wt% Pt, 10 wt% Ru, Johnson Matthey, UK) and Pt/C (20 wt% Pt, Johnson Matthey, UK) were used as anode and cathode catalysts, respectively. The catalysts were mixed with deionized water, Nafion® ionomer solution (5 wt%, Aldrich), and isopropyl alcohol in an ultrasonic bath at ambient temperature for 30 min to obtain homogeneous catalyst inks. Carbon papers (Toray; 10 and 20 wt% Teflonized) were used as anode and cathode diffusion layers, respectively. The catalyst inks were separately spread on each of the Teflonized carbon paper diffusion layers, and these were then treated with a 5000 V cm^{-1} ac electric field of a specific frequency (0.1, 1.0, or 10.0 Hz) under vacuum-drying at 110 °C for 1 h to form anodic or cathodic electrodes. To apply the electric field, the diffusion layers with catalyst inks were placed in the narrow gap between two parallel metal electrodes, which were connected to a high-voltage power source (HVA-252NP5, China). The anodic and cathodic electrodes were separately placed on either side of a pretreated Nafion® 115 (Du Pont) membrane, and then hot-pressed at 10 MPa and 120 °C for 120 s to form an MEA with an active area of 4 cm^2. The MEAs thus prepared are denoted as E-MEA1, E-MEA2, or E-MEA3, corresponding to the frequencies of 0.1, 1.0, or 10.0 Hz of the applied ac electric field. The MEA prepared under the same conditions but without applying an electric field is denoted as C-MEA.

For each MEA prepared for this study, the Pt loadings were 2.0 mg cm^{-2} in the anode and 1.0 mg cm^{-2} in the cathode, and the Nafion® ionomer content was 20 wt% in both the anode and cathode.

Separate cathodic catalyst layers (CLs) were also prepared for the purpose of easy characterization. The CLs had chemical compositions identical to those of the cathodes of the MEAs prepared for this study. These, denoted as E-CL1, E-CL2, E-CL3, and C-CL, were prepared under the same conditions as the corresponding E-MEA1, E-MEA2, E-MEA3, and C-MEA, respectively, except that the separate

CLs were made by spreading catalyst inks on epoxy plates rather than on carbon papers. The insulating and planar epoxy plates supported the CLs mechanically, thereby enabling measurement of the conductivity of the CLs alone, without interference from the carbon paper.

2.2. MEA characterizations

The electrochemical impedance spectra (EIS) of the whole MEAs and the anodes were separately measured by using a PGSTAT20 potentiostat/frequency response analyzer from Autolab (The Netherlands). The EIS of the MEAs were obtained under conditions of a flow of 1 mol L^{-1} aqueous methanol solution at 100 mL min^{-1} to the anodes and a flow of oxygen at 100 mL min^{-1} to the cathodes. To obtain the EIS of the anodes, hydrogen at a rate of 100 mL min^{-1} was sent to the cathodes, which in this case acted as both the reference and counter electrodes. In both cases, scanning was carried out from high to low frequencies over the range 4000–0.01 Hz, with the amplitude of the sinusoidal potential signal being 10 mV. The EIS were analyzed with regard to equivalent circuits by using Autolab FRA version 4.9.006 circuit-fitting software.

The in-plane ionic and electronic resistances of the cathodic catalyst layers were obtained from their EIS measured by the aforementioned PGSTAT20 potentiostat/frequency response analyzer. The measurement used a 10 mV sinusoidal potential signal in the frequency range 0.1–10^6 Hz, and was carried out at room temperature and 100% relative humidity. The in-plane electronic resistance R_e and ionic resistance R_i of the CLs were derived from equivalent circuit fittings, as detailed in refs. [14,15].

The electrochemical surface area (ESA) of the cathode in different MEAs was determined by cyclic voltammetry (CV) (Autolab PGSTAT20, The Netherlands). The cathode was fed with N$_2$-purged deionized water at a rate of 1.0 mL min^{-1}, while the anode was fed with 0.1 MPa humidified hydrogen at 100 mL min^{-1} and thereby served as a dynamic hydrogen electrode (DHE). CV curves were obtained by scanning in the range 0–1.2 V (vs. DHE) at a rate of 20 mV s^{-1}. The integrated peak area of hydrogen desorption (0.05–0.4 V vs. DHE) was used to calculate the ESA of the cathode catalysts.

A Philips XL30 scanning electron microscope (SEM) was employed to observe the microstructure and morphology of the catalyst layers in MEAs. Fresh cross-sectional cryogenic fractures of the MEAs were vacuum sputtered with a thin layer of Au prior to SEM examination.

2.3. Single cell test

The DMFC performance of the MEAs was tested by using an in-house single fuel cell test set-up. The MEA to be tested was sandwiched between two thick graphite plates with flow channels. A 1 mol L^{-1} aqueous methanol solution was fed to the anode channel at 1 mL min^{-1} by means of a peristaltic pump. Humidified oxygen gas was fed to the cathode channel at 100 mL min^{-1} and 0.1 MPa. The DMFC test was operated at 80 °C.

3. Results and discussion

When exposed to an electric field, dispersed polarizable particles tend to attract one another and line-up in the direction of the field, as a result of dipole–dipole interactions. This has been observed in various dispersed systems by different researchers. Our catalyst ink resembles such dispersed systems, because the Pt/C or Pt-Ru/C particles should be fully polarized in an electric field. Consequently, the application of a sufficiently strong electric force to
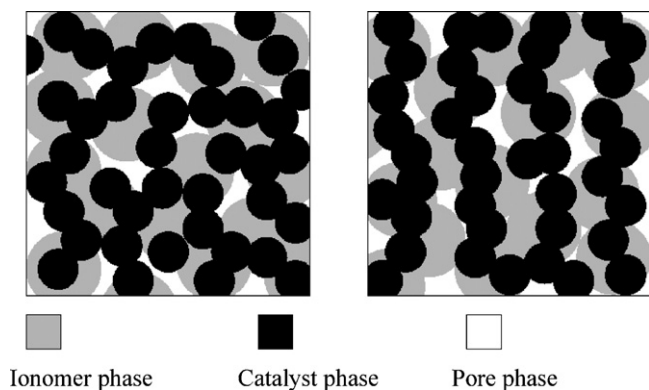
Fig. 1. Schematic representation of random (left) and aligned (right) catalyst layers.

a CL in its trans-plane direction will align the dispersed Pt/C or Pt-Ru/C particles, thereby leading to decreased trans-plane electronic resistance in the CL (Fig. 1).

However, due to the very thin form of a CL, accurate measurement of its trans-plane electronic resistance is hard to achieve, as the contact resistance between the measuring electrode and the CL can be of the same order of magnitude. Fortunately, the changes in the in-plane electronic resistance of a CL are related to the alignment in the trans-plane direction. The alignment of the electronically conductive particles would cause both a decrease in the resistance in the aligning direction, and an increase in the other two directions, which is due to the fact that the particles occupy only a part of the total space of the CLs (Fig. 1). A perfect alignment of the catalyst particles in the trans-plane direction would result in the electronic resistance of the CL approaching the minimum in the trans-plane direction and approaching infinity in the in-plane direction. Therefore, we turned our attention to measuring the changes in the in-plane resistance, in order to identify any sign of alignment in the CLs as a result of application of the trans-plane electric field.

The results of in-plane resistance measurements of the different CLs are shown in Fig. 2. The corresponding electronic resistances R_e and ionic resistances R_i of these CLs obtained by equivalent circuit fitting are summarized in Table 1. The equivalent circuit adopted was identical to that in Ref. [14]. As can be seen from Table 1, the in-plane electronic resistances R_e of the three E-CLs are markedly higher than that of the C-CL. This result is in accordance with our aforementioned analysis and indicates a certain degree of trans-plane alignment or orientation.

It is also evident from Table 1 that the in-plane ionic resistances of the three E-CLs are also considerably higher than that of the C-CL. This, too, indicates trans-plane orientation, and thus lowered resistance of the ion-conductive phase in the CL, which is a welcome attribute, as it will lead to improved fuel cell performance. However, the orientation of the ionomer phase seems to be more complicated, for it is a continuous phase in the catalyst ink, at least at the beginning of its exposure to the electric field. However, there may be a period in which phase separation of the ionomer solution occurs with the evaporation of solvent [16]. In such a period, dispersed ionomer aggregates will have a chance to align if exposed to an appropriate electric field. This might also happen as a ramification of the alignment of the electronically conductive phase. That
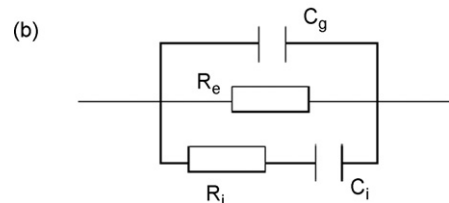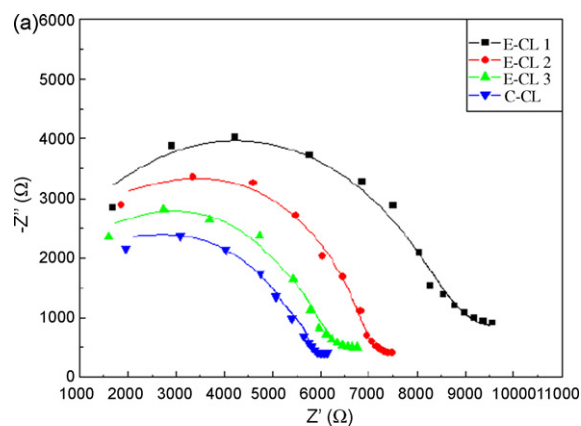

Fig. 2. (a) In-plane EIS experiment (dots) and fitting (lines) results of the CLs at 25 °C and 100% RH. E-CL1, E-CL2, and E-CL3 signify catalyst layers exposed to 0.1, 1.0, and 10 Hz ac electric fields, while C-CL corresponds to that not exposed to an electric field. (b) The equivalent circuit of the CLs for in-plane impedance fitting. Subscript notation: e, electronic, i, ionic, g, geometric.

is to say, the ionomer is attached to the aligned Pt/C or Pt-Ru/C, so that it also aligns. These possibilities need to be verified through further investigations.

The decreases in the trans-plane mixed resistances of the different E-MEAs are presented in Figs. 3 and 4 and Tables 2 and 3. The equivalent circuits adopted in modeling the anodes of the MEAs (Fig. 3b) and the whole MEAs (Fig. 4b) were similar to those used
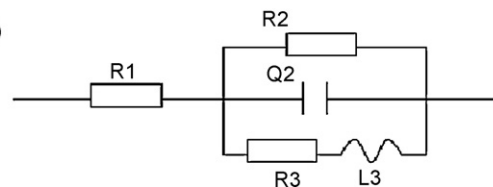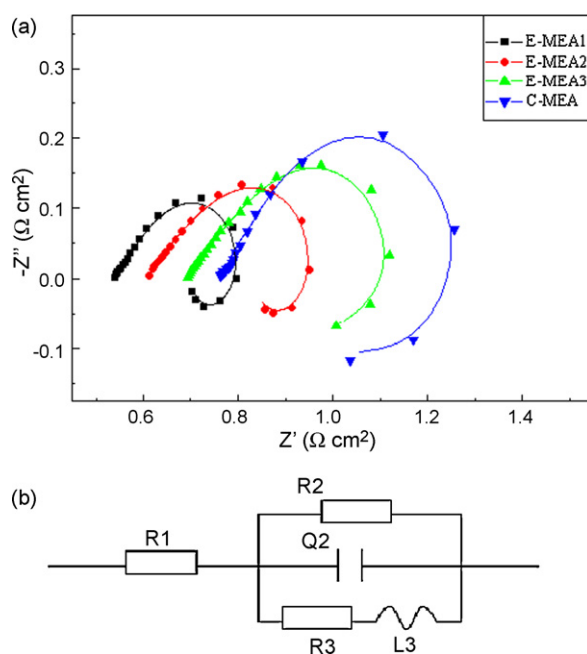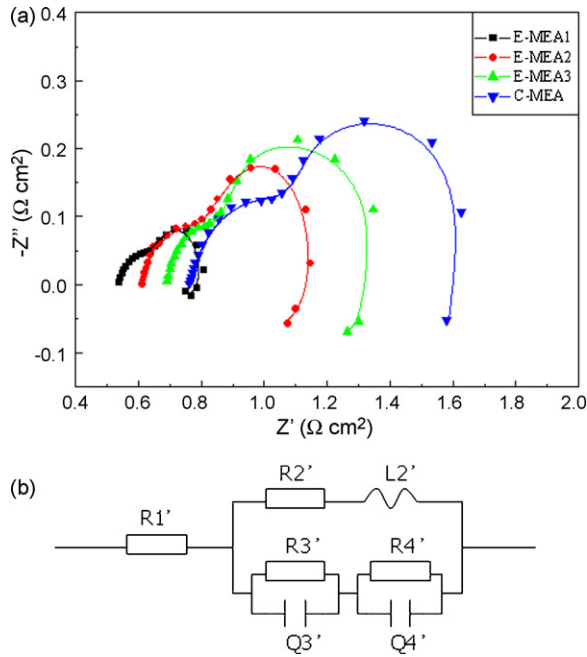

Fig. 3. (a) Experimental (dots) and fitting (lines) EIS results of different MEA anodes at 100 mA cm^{-2} and 80 °C (The anode was fed with 1 mol L^{-1} CH$_3$OH at 1 mL min^{-1}, while the cathode was fed with H$_2$ at 0.1 MPa and 100 mL min^{-1}). (b) The equivalent circuit adopted for anode EIS fitting.

Table 1
In-plane ionic and electronic resistances obtained according to results from Fig. 2.

	E-CL1	E-CL2	E-CL3	C-CL
R_e (Ω)	9,123	7,558	6,663	6,099
R_i (Ω)	96,710	76,810	53,070	43,820

Fig. 4. (a) Experimental (dots) and fitting (lines) EIS results of different MEAs at $100\,mA\,cm^{-2}$ and $80\,^{\circ}C$ (the anode was fed with $1\,mol\,L^{-1}$ CH_3OH at $1\,mL\,min^{-1}$, while the cathode was fed with O_2 at $0.1\,MPa$ and $100\,mL\,min^{-1}$). (b) The equivalent circuit adopted for MEA EIS fitting.

Table 2
Parameter values of the circuit elements in Fig. 3.

	E-MEA1	E-MEA2	E-MEA3	C-MEA
$R1$ ($\Omega\,cm^2$)	0.540	0.613	0.693	0.764
$R2$ ($\Omega\,cm^2$)	0.992	1.371	2.462	3.813
$Q2-Y_0$ ($\Omega^{-1}\,cm^{-2}\,s^{-n2}$)	2.426	2.039	1.781	1.262
$Q2-n$	0.569	0.640	0.665	0.699
$R3$ ($\Omega\,cm^2$)	0.197	0.204	0.286	0.317
$L3$ ($H\,cm^2$)	0.264	0.427	0.732	1.222
Anode reaction resistance ($\Omega\,cm^2$)	0.164	0.178	0.256	0.293

Note: $R1$ is the mixed electronic and ionic resistance of the membrane and catalyst layers. $R2$ is the methanol oxidation resistance. $R3$ is oxidation resistance of CO_{ads}. $L3$ is the inductance due to the relaxation of CO_{ads} coverage. $Q2$ is the constant phase angle element, which has the impedance $Z_Q = Y_0^{-1}\,(j\omega)^{-n}$.

in refs. [17,18]. The mixed resistance $R1$ or $R1'$ of an MEA consists of the resistances from the two catalyst layers and that from the membrane. Because the membranes were identical in the different E-MEAs and C-MEA, any changes in the mixed resistances should

Table 3
Parameter values of the circuit elements in Fig. 4.

	E-MEA1	E-MEA2	E-MEA3	C-MEA
$R1'$ ($\Omega\,cm^2$)	0.542	0.618	0.699	0.771
$R2'$ ($\Omega\,cm^2$)	0.243	0.385	0.504	0.817
$L2'$ ($H\,cm^2$)	0.872	1.051	1.648	2.344
$R3'$ ($\Omega\,cm^2$)	1.176	2.126	3.296	5.371
$Q3'-Y_0$ ($\Omega^{-1}\,cm^{-2}\,s^{-n3'}$)	2.208	1.967	1.543	1.167
$Q3'-n$	0.628	0.672	0.716	0.729
$R4'$ ($\Omega\,cm^2$)	0.118	0.166	0.236	0.313
$Q4'-Y_0$ ($\Omega^{-1}\,cm^{-2}\,s^{-n4'}$)	0.466	0.381	0.304	0.262
$Q4'-n$	0.731	0.802	0.855	0.896
Total reaction resistance ($\Omega\,cm^2$)	0.205	0.330	0.441	0.714

Note: $R1'$ is the mixed electronic and ionic resistance of the membrane and catalyst layers. $R2'$ is the oxidation resistance of CO_{ads}. $L2'$ is the inductance due to the relaxation of CO_{ads} coverage. $R3'$ is the methanol oxidation resistance. $R4'$ is the oxygen reduction resistance. $Q3'$ and $Q4'$ are the constant phase angle elements, which have the impedance $Z_{Qi} = Y_{0i}^{-1}(j\omega)^{-ni}$.
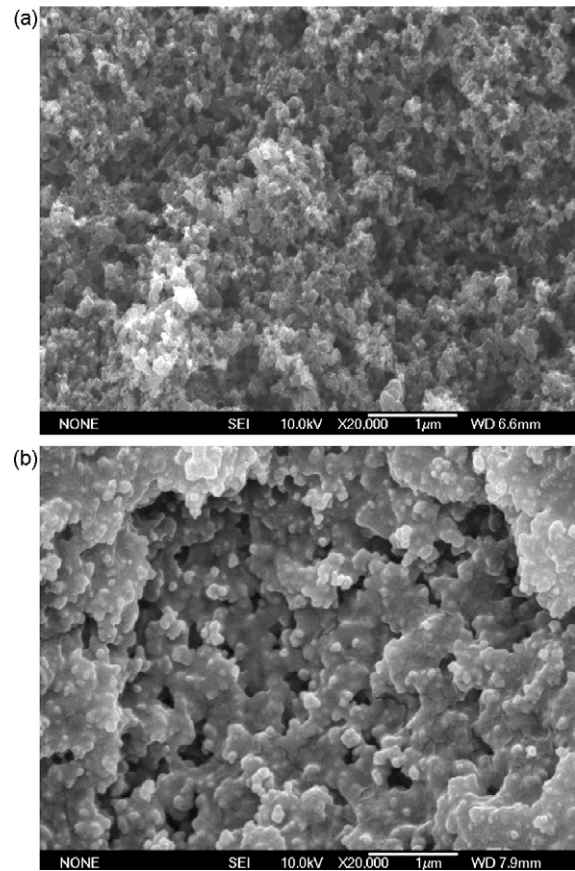

Fig. 5. Cross-section SEM images of (a) E-MEA1 and (b) C-MEA cathode catalyst layers.

be solely attributable to that of their catalyst layers. Moreover, the decrease in the mixed resistance should derive from both the electronic and ionic conductive phases of the catalyst layers, because of the increased in-plane resistances in both phases (Fig. 2 and Table 1).

However, SEM images of the electric field-treated catalyst layers showed little sign of alignment (Fig. 5a). A possible reason for this was that the alignment was still far from approaching its full extent under the applied experimental conditions. It may also be the case that rotation of the metal-on-carbon catalyst particles constitutes a significant part of the orientation, which alters trans-plane and in-plane resistances but is visually undetectable. Clearly, these speculations call for more in-depth investigations.

Despite providing no evidence for alignment, the SEM images do show noticeable morphological differences between E-CL and C-CL (cf. Fig. 5a and b). In contrast to the large blocks of solid phase and uneven pores in the common catalyst layer, both the pore and solid phases in the electric field-treated catalyst layer looked finely and evenly distributed. The repulsive force between like charges is likely to explain the smaller size of the solid aggregates to a certain degree, if we compare the E-CL with ultrathin fibers made by an electrospinning process [19]. Moreover, the applied electric field may have other effects, e.g. polarization of the solvent in the catalyst ink, which in turn could affect the morphology of the CL formed.

The decrease in the reaction resistances of the E-MEAs, as compared with C-MEA, is another obvious consequence of the electric field treatment. The anode reaction resistance consists of the methanol oxidation resistance $R2$ (or $R3'$) and the oxidation resistance of adsorbed carbon monoxide $R3$ (or $R2'$), while the total reaction resistance is composed of the anode reaction resistance
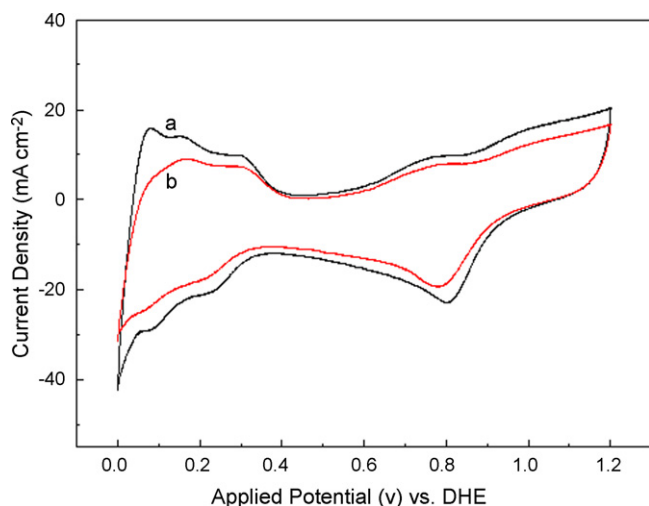
Fig. 6. CV curves of (a) E-MEA1 cathode and (b) C-MEA cathode obtained at $20\,mV\,s^{-1}$ sweep rate.

Fig. 7. V–I and P–I curves of DMFC with different MEAs. The fuel cell was run at 80 °C, with the anode being fed with $1\,mol\,L^{-1}$ CH_3OH at $1\,mL\,min^{-1}$ and the cathode being fed with O_2 at 0.1 MPa and $100\,mL\,min^{-1}$.

and the cathodic oxygen reduction resistance $R4'$. According to the data in Table 2, the anode reaction resistance decreased by 87%, 61%, and 56%, respectively, as a result of treatment with electric fields of the various frequencies. Similarly, the total reaction resistance was reduced by 62%, 46%, and 29%, respectively, under the same electric field treatments (Table 3). These results are consistent with the SEM observation, which showed that the electric field-treated catalyst layer had smaller sized solid aggregates and more evenly distributed pores (Fig. 5). In other words, more catalyst particles are located at the surface and those in the inner part of the aggregates become easier to reach by the reactants. In this case, the catalyst layers should display low reaction resistances as a result of high ESA and low mass-transfer resistance.

Cyclic voltammetry measurements provided more direct evidence of an increased ESA for E-MEAs as compared to C-MEA. Two CV curves for the E-MEA1 and C-MEA cathodes, respectively, are shown in Fig. 6. With the assumption that the specific quantity of charge for the electro-oxidation of an adsorbed hydrogen monolayer on the Pt surface was $210\,\mu C\,cm^{-2}$ [20], the ESAs were calculated using the hydrogen desorption peaks in the lower potential region between 0.05 and 0.4 V vs. DHE. An ESA of $87.0\,m^2\,g^{-1}$ was derived for E-MEA1, as opposed to $51.3\,m^2\,g^{-1}$ for C-MEA, indicating an increment of almost 70% in ESA as a result of the electric field treatment. Adopting the estimate of $140\,m^2\,g^{-1}$ for the specific surface area of 20 wt% Pt on carbon from Johnson Matthey [21], it can be seen the catalyst utilization increased from around 37–62%.

The MEAs prepared under different conditions were also compared by testing their V–I polarization curves in a direct methanol fuel cell (DMFC) (Fig. 7). The E-MEAs show enhanced performance in terms of open-circuit voltage and the peak output power density as compared with the C-MEA. An increase of 12–42% in peak output power density was achieved in the DMFC by using the E-MEAs. It is noticeable that the electric field-treated MEAs in the DMFC present higher voltages over the whole range of output currents, and that the voltage difference becomes larger in the high current region. The enhanced DMFC performance of the E-MEAs is consistent with the EIS, SEM, and CV results, which reveals improved electronic and ionic connections and increased ESA in the electric field-treated catalyst layers.

The frequency of the ac electric field was seen to have noticeable effects on the E-CLs or E-MEAs prepared, as indicated by the variation in their in-plane and trans-plane resistances (Figs. 2–4) and DMFC performance (Fig. 7). Under the specified experimen-
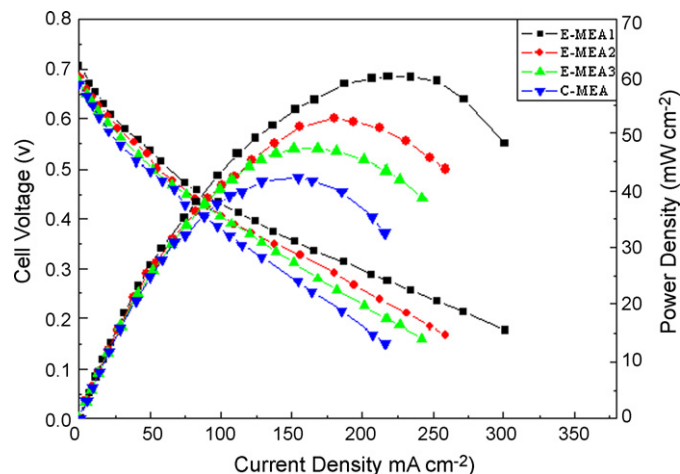
tal conditions, the electric field of lower frequency always resulted in a higher degree of alignment in the catalyst layer. The polarization of the electronically conductive metal-on-carbon particles should be instantaneous, but the process of aligning the particles may be slow in the viscous ionomer solution. On the other hand, the electric field driven stretching and conglomerating of dispersed ionomer may also be slow because of its viscosity. Therefore, a very low frequency ac electric field may be more effective in inducing alignment of the particles by allowing them sufficient time to move. In addition, the strength of the dipole–dipole interaction may be a function of the field frequency [22], so that the attraction between the particles may be stronger at low frequency, thereby leading to a higher degree of alignment. However, these speculations have yet to be verified and further investigation is needed to elucidate the effects of field frequency on the E-MEAs.

4. Conclusions

To improve the performance of PEM fuel cells, MEAs have been prepared under treatment with an ac electric field. Enhanced performance of the electric field-treated MEAs has been verified through DMFC experiments, with increases in peak output power density of 12–42% compared with the MEA not treated with an electric field. Under the experimental conditions of this study, more obvious enhancement in the performance of the ac electric field-treated MEAs was observed for a lower ac field frequency. Two consequences of the electric field treatment have been observed through EIS, SEM, and CV characterizations of the MEAs. First, both the electronic and ionic phases in the catalyst layers are aligned to certain extent, which results in improved electrical connections in the trans-plane direction. Second, the solid-phase aggregates and the pores in the catalyst layer are finely distributed, which leads to increased ESA and decreased reaction resistance. However, there are still many issues to resolve and unexplored factors concerning the electric field treatment. Further investigation is ongoing in our laboratory.

References

[1] S.M. Haile, Acta Mater. 51 (2003) 5981.
[2] T. Schultz, K. Sundmacher, J. Membr. Sci. 276 (2006) 272.
[3] D. Kim, J. Lee, T.H. Lim, I.H. Oh, H.Y. Ha, J. Power Sources 155 (2006) 203.
[4] J.H. Kim, H.Y. Ha, I.H. Oh, S.A. Hong, H.N. Kim, H.I. Lee, Electrochim. Acta 50 (2004) 801.
[5] R. Fernandez, P.F. Aparicio, L. Daza, J. Power Sources 151 (2005) 18.
[6] F.Q. Liu, C.Y. Wang, Electrochim. Acta 52 (2006) 1417.
[7] C.Y. Du, G.P. Yin, X.Q. Cheng, P.F. Shi, J. Power Sources 160 (2006) 224.
[8] E. Muth, Kolloid. Z. 41 (1927) 97.
[9] Y. Oren, V. Freger, C. Linder, J. Membr. Sci. 239 (2004) 17.
[10] H.L. Lin, T. Leon Yu, F.H. Han, J. Polym. Res. 13 (2006) 379.
[11] M.K. Schwarz, W. Bauhofer, K. Schulte, Polymer 43 (2002) 3079.
[12] H.Q. Wang, H.Y. Zhang, W.F. Zhao, W. Zhang, G.H. Chen, Compos. Sci. Technol. 68 (2008) 238.
[13] E. Middelman, Fuel Cells Bull. 2002 (2002) 9.
[14] A.P. Saab, F.H. Garzon, T.A. Zawodzinski, J. Electrochem. Soc. 149 (2002) A1541.
[15] A.P. Saab, F.H. Garzon, T.A. Zawodzinski, J. Electrochem. Soc. 150 (2003) A214.
[16] H. Li, S. Schlick, Polymer 36 (1995) 1141.
[17] M.K. Jeon, J.Y. Won, K.S. Oh, K.R. Lee, S.I. Woo, Electrochim. Acta 53 (2007) 447.
[18] J.T. Müller, P.M. Urban, W.F. Hölderich, J. Power Sources 84 (1999) 157.
[19] A. Frenot, I.S. Chronakis, Curr. Opin. Colloid Interf. Sci. 8 (2003) 64.
[20] A. Pozio, M.D. Francesco, A. Cemmi, F. Cardellini, L. Giorgi, J. Power Sources 105 (2002) 13.
[21] E.A. Ticianelli, C.R. Derouin, S. Srinivasan, J. Electroanal. Chem. 251 (1988) 275.
[22] L.D. Landau, E.M. Lifshitz, Electrodynamics of Continuous Media, Pergamon, New York, 1984.